Nuclear Inst, and Methods in Physics Research B 430 (2018) 42–46

Contents lists available at ScienceDirect

Nuclear Inst. and Methods in Physics Research B

journal homepage: www.elsevier.com/locate/nimb

Fluence dependent changes of surface morphology and sputtering yield of iron: Comparison of experiments with SDTrimSP-2D

R. Stadlmayr[a,*], P.S. Szabo[a], B.M. Berger[a], C. Cupak[a], R. Chiba[a,1], D. Blöch[a], D. Mayer[a], B. Stechauner[a], M. Sauer[b], A. Foelske-Schmitz[b], M. Oberkofler[c], T. Schwarz-Selinger[c], A. Mutzke[d], F. Aumayr[a]

[a] Inst. of Applied Physics, TU Wien, Fusion@ÖAW, Wiedner Hauptstraße 8-10, 1040 Vienna, Austria
[b] Analytical Instrumentation Center, TU Wien, Getreidemarkt 9, 1060 Vienna, Austria
[c] Max-Planck-Institut für Plasmaphysik, Bolzmannstraße 2, 85748 Garching, Germany
[d] Max-Planck-Institut für Plasmaphysik, Wendelsteinstraße 1, 17491 Greifswald, Germany

ARTICLE INFO

Keywords:
Sputtering
Erosion
Quartz-crystal-microbalance
Surface roughness
Trim

ABSTRACT

The influence of surface morphology modifications on the sputtering yield of thin Fe films by monoenergetic Ar ions is studied by using a highly sensitive quartz crystal microbalance (QCM) technique. The morphology changes are induced by prolonged sputtering up to a total Ar fluence of 8×10^{21} m^{-2}. Atomic force microscopy (AFM) measurements are performed to analyse the sample topography before and after irradiation and to determine surface roughness parameters. Numerical modelling with the codes SDTrimSP and SDTrimSP-2D are performed for comparison. Our investigations show that by using the local distribution of projectile impact angles, as derived from AFM measurements, as well as the elemental composition of the samples as an input to the codes SDTrimSP and SDTrimSP-2D the agreement between experiment and simulations is substantially improved.

1. Introduction

Ion induced sputtering is one of the most important topics of ion-surface interaction and has a wide variety of practical applications, like surface cleaning, etching, thin-layer deposition or surface analytic techniques. Sputtering also plays a major role in erosion of wall material in nuclear fusion devices [1] or in space weathering by solar wind ion impact observed on lunar or planetary surfaces [2,3]. Plasma facing components (PFC) in a fusion device are constantly eroded by ion and neutral particle bombardment, which limits their lifetime. For a future fusion power plant tungsten is foreseen as material for PFCs and tungsten containing steels, like EUROFER are considered as possible alternatives for recessed area PFCs in the reactor vessel [4]. Experiments with Fe-W films (with 1.5 at% W), which is assumed to be a model system for EUROFER (nominally 0.33 at% W), showed a significant reduction of the erosion rate during low energy ion bombardment [5]. The reduced erosion rate was explained by preferential sputtering of Fe, causing a W surface enrichment. However modifications of the surface structure due to erosion were measured in addition [6], which also influence the sputtering behaviour. In order to separate the effect of surface enrichment of high Z materials from the effect of surface structural modifications, we set out to conduct sputtering experiments with pure Fe sample films and investigated the effect of surface morphology changes on the sputtering yield due to prolonged ion erosion.

Theoretical descriptions (e.g. [7]) and simulations (e.g. [8]) of sputtering often only consider perfectly flat surfaces. However, this is an idealization, and while it is possible to create reasonably flat films for some materials, this assumption will often lead to discrepancies with the actual experimental conditions. Fig. 1 shows a sketch of how the roughness of a surface may affect the sputtering process. It shows a projectile ion hitting the surface under a nominal angle of 0 degrees, which would mean normal incidence for a perfectly flat surface. However, due to the rough surface condition the local angle of incidence θ is different, with its value being strongly dependent on the exact point of incidence. Beside surface sputtering also projectile reflection may occur. Sputtered target atoms are assumed to follow a cosine distribution with its maximum in the direction of the local surface normal. Experiments have shown, that the sputtering yield as a function of local impact angle Y (θ) follows more a $\cos^y(\theta)$ distribution,

* Corresponding author.
E-mail address: stadlmayr@iap.tuwien.ac.at (R. Stadlmayr).
[1] Present address: Tokyo Institute of Technology, Meguro-ku, Tokyo 152-8550 Japan.

https://doi.org/10.1016/j.nimb.2018.06.004
Received 6 October 2017; Received in revised form 24 April 2018; Accepted 6 June 2018

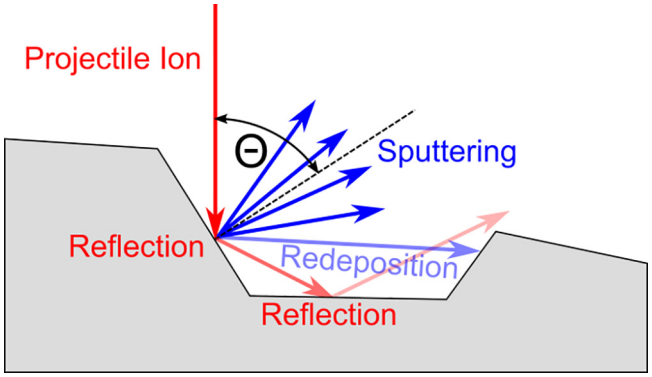

Fig. 1. Sputtering of a rough surface. A projectile ion, which is represented by the red arrow, hits a surface under nominal normal incidence. However due to the surface structure the local angle of incidence θ differs from 0 degree and thus affects the sputtering yield. Some of the sputtered atoms cannot escape the surface and get redeposited, while multiple reflections of the projectile ion may lead to further erosion of the surface (after [10]).

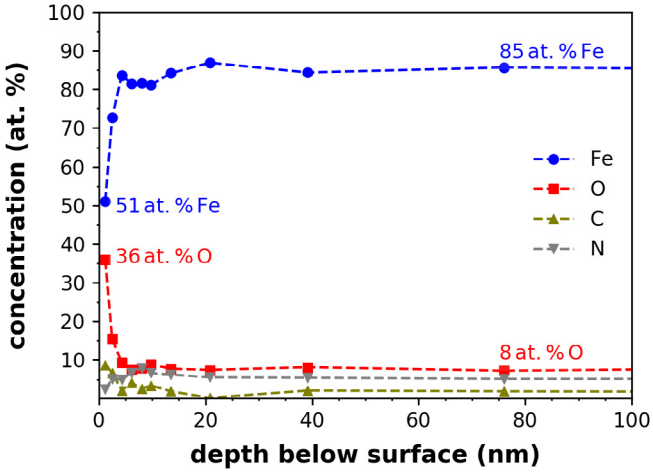

Fig. 2. The XPS analysis of the Fe-film as function of depth shows a significant oxide layer on top of the sample.

where y is frequently greater than 1 [9]. As is indicated in Fig. 1, not all of the sputtered atoms are able to escape the surface. Some of them may hit other parts of the rough surface and could be deposited there. Additionally, the projectile is reflected with a certain probability and may hit the surface a second time. The energy of the reflected projectile is lower than the incident energy, but might still be high enough to lead to further sputtering. These sputtered particles are then again partly redeposited (omitted in Fig. 1 for clarity) and with a given probability further reflection may occur.

Evidently, a theoretical description of the sputtering of rough surfaces becomes quite complex. Küstner et al. achieved remarkable results using STM images as an input and a simple model to describe redeposition effects ([10,11]). However, more detailed modelling of this situation is necessary to take into account effects such as shadowing (especially for flat ion incidence some parts of the surface will not be accessible to the ions) and the change in angular and energy distributions, where Fig. 1 already indicates large changes compared to a flat surface. For this reason, we have used the recently developed SDTrimSP-2D code [12,13] to take the actual surface structure into account in the sputtering simulations and compare the results of the simulations to our experimental data.

2. Experimental approach

The measurements have been performed using a highly sensitive quartz crystal microbalance (QCM) developed at TU Wien and described in more detail in [14,15]. This setup is an ideal tool to measure small mass changes and allows in-situ investigation of a dynamic erosion behaviour [6,16]. Our investigations concentrated on mono-energetic Ar ions of 500 eV hitting on an Fe-coated QCM sample. Ar might be used as seeding gas in fusion reactors like ITER, to avoid local overheating of the PFCs by radiative cooling [17]. Additionally Ar - > Fe sputtering yields are significantly higher than D – > Fe sputtering yields, making Ar^+ projectiles ideally suited for our experiments.

Typically 400 nm thin Fe films were deposited onto polished quartz crystals, by using a magnetron sputter deposition apparatus at IPP Garching, Germany. As the QCM technique only allows the measurement of the total mass change of the quartz and the presence of an oxide layer on the Fe film was assumed, one of the Fe films was analysed by X-Ray Photoelectron Spectroscopy (XPS). Sputter depth profiling via Ar-ion sputtering in combination with XPS was used to obtain the quantitative elementary analysis as a function of depth. This measurements were conducted on a custom SPECS XPS system with a monochromatized Al K-alpha source (μFocus 350) and a wide-angle lens hemispherical analyser (WAL 150).

XPS results are given in Fig. 2 and show a high concentration of O at the surface indicating a native oxide layer as expected. Long term sputtering shows that the Fe concentration only reaches 85% in the bulk of the film and substantial concentrations of O, N and C are still detected in the XP spectra. We will show below, that for the simulations it is essential to take the actual elemental composition into account.

The evolution of the sputtering behaviour of the Fe model films under Ar ion bombardment was then investigated at the specific angle of incidence of $\alpha = 60$ degree and in dependence of the bombarding ion fluence (results are shown in Section 4). Measurements were performed at an Ar ion flux of $\approx 5 \times 10^{16}\,m^{-2}\,s^{-1}$ and at an Ar base pressure of 1×10^{-7} mbar.

AFM images of the Fe-coated quartz crystal samples were taken before and after prolonged irradiation (see Fig. 3a and b). On the initial surface, nano-scale structures are visible (Fig. 3a) that significantly change during the ion bombardment. For example after application of a total Ar fluence of $8 \times 10^{21}\,m^{-2}$ under an angle of incidence of 60 degree a structure strongly aligned with the incoming projectile direction becomes visible (Fig. 3b).

3. Modelling with SDTrimSP

SDTrimSP is a Monte Carlo code that allows the simulation of ions hitting a solid target based on the binary collision approximation (BCA) [8]. It represents a dynamic enhancement of the widely used “static” TRIM code [19] and the dynamic code TRIDYN [20,21]. In the dynamic mode composition and thickness changes of the sputter target are included, while in the static mode these changes are suppressed. In addition the code allows parallel computing, which reduces computing time. SDTrimSP results perform very well for calculating sputtering yields especially compared to the SRIM code [22,23]. The target in a SDTrimSP calculation is set up one-dimensionally, where several discrete layers of different compositions can be defined. This means that only depth-dependent aspects of the target’s change due to particle bombardment can be taken into account.

The two-dimensional expansion SDTrimSP-2D developed at the Max Planck Institute for Plasma Physics (IPP) allows implementing a surface structure into an SDTrimSP simulation [12]. This is realized by expanding the geometrical description from layers to a grid, where the cell modification is calculated from the material transport following the collision cascades. Surface cells can grow and shrink based on the transport of target atoms and thus a change in the surface morphology can be simulated. First results presented in [24] confirmed the validity of the model and reproduce experimental observations precisely.

The surface topography of our Fe films as deduced from the AFM

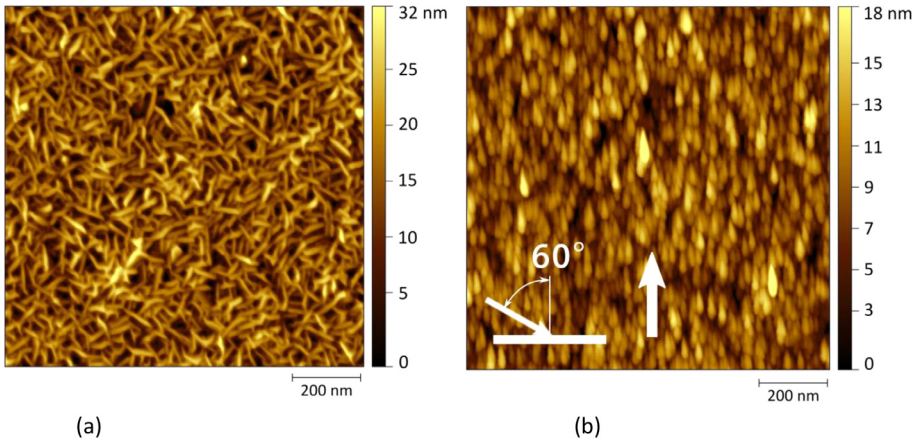

Fig. 3. AFM images of the target before (a) and after (b) ion irradiation with a total Ar fluence of 8×10^{21} m^{-2} show a significant change of the surface structure. An initial nano-scale structure on an unirradiated sample transforms into a structure clearly aligned in the direction of irradiation (indicated by the white arrow) [18].

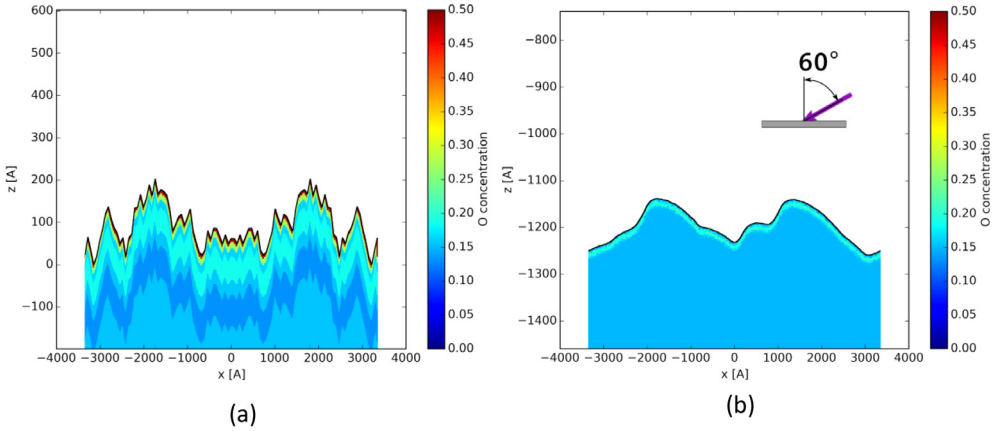

Fig. 4. (a) The model surface used as input for the SDTrimSP-2D simulations. The color represents the O concentration in the respective depth. The x-axis represent the lateral positon along the surface and the z-axis the depth relative to the unirradiated surface. The surface was defined to have the same distribution of local impact angles and RMS value as derived from the AFM image in Fig. 3a. (b) After irradiation with 500 eV Ar ions up to a total Ar fluence of 8×10^{21} m^{-2} impinging under a nominal angle of incidence of 60 degree from the right, the simulations show a smoothening of the surface consistent with the experimental data presented in Fig. 3. Additionally oxygen depletion at the surface occurs.

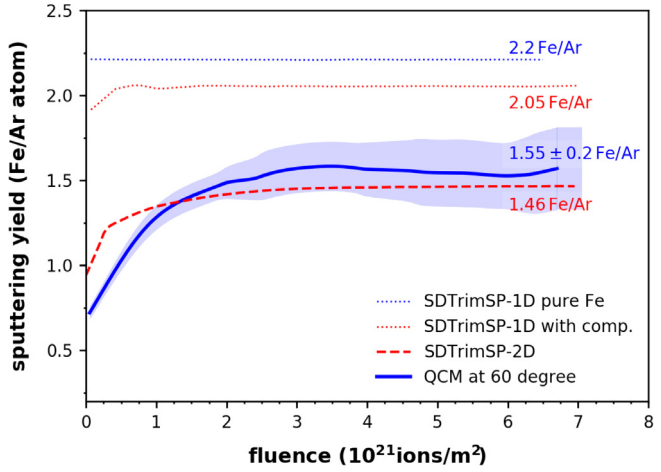

Fig. 5. Measured sputtering yield for 500 eV Ar ions bombarding an iron film under an angle of incidence of 60 degree, as a function of the Ar ion fluence (thick blue line). The increase of the sputtering yield at low fluences corresponds to the sputtering of the oxide layer. The dotted and dashed lines represent numerical simulations with SDTrimSP-1D and 2D. Taking into account the actual elemental composition of the target improves the 1D-simulation (red dotted line) somewhat. By including the surface morphology in a SDTrimSP-2D simulation (thick red dashed line) the agreement with experimental results is substantially improved.

measurements (Fig. 3) was used as an input for SDTrimSP-2D. However, the AFM images in Fig. 3 clearly show a structure that cannot easily be reduced to two dimensions without omitting important information about the surface. Taking one line of (x, z)-coordinates of the AFM image would, for example, result in a surface that would appear much flatter because any additional inclination in y-direction would be ignored. For this reason an initial 2D target was defined which has the same RMS roughness value as the real sample and the same distribution of the "local impact angles θ" (cf. section 4). This distribution shows the range of impact angles between the local surface normal and projectile incidence direction (see Fig. 1). A target consisting of 10 initial layers with different concentrations of Fe and O according to the elemental composition retrieved from the XPS analysis (see Fig. 2) was set up. Additionally the compound option was used in SDTrimSP-2D, to take into account the density and surface binding energy for iron(III)-oxide (data taken from [25]). The final target surface that was used as a starting point for the SDTrimSP-2D simulations is shown in Fig. 4a, with the color scale denoting the O concentration.

Using this model target, SDTrimSP-2D simulations with 500 eV Ar were performed. On the one hand, the fluence dependence of the sputtering yield as well as the change of the surface morphology during the irradiation was simulated. On the other hand, the angular dependence of the sputtering yield before and after these irradiations was investigated. The results of these simulations are presented in the following section and compared to the experimental data.

4. Comparison of experimental results to SDTrimSP-1D and SDTrimSP-2D

Fig. 5 shows the measured fluence dependent sputtering yield of the Fe coated QCM sample when irradiated by 500 eV Ar ions at an angle of incidence of 60 degree. The sputtering yield increases from 0.7 Fe

atoms per incident Ar ion to 1.5 Fe atoms per incident Ar ion and reaches steady state after an Ar fluence of about 2–3 × 10^{21} m^{-2}. It should be noted, that the QCM technique allows measuring the total mass change rate only. The resulting mass change rate is then divided by the molar mass of Fe to scale it to the sputtering yield of Fe [14]. The observed initial strong change of the sputtering yield is due to the removal of an oxide layer, while changes at higher fluences can be attributed to the change in surface morphology/roughness. The SDTrimSP-1D simulation assuming a target with pure Fe shows no fluence dependence and a constant sputtering yield of 2.2 Fe atoms per incident Ar ion, which is higher than the actual measurements. A detailed analysis of our simulation results show that the main reason for this discrepancy can be found in the C, N and O concentrations of the sample neglected in this 1D simulation. If the SDTrimSP-1D simulation includes the elemental depth distribution, as measured with XPS, the resulting sputtering yield is closer to the experimental data, but still too high and the transient effect at very low fluences is not well reproduced. It should be noted, that the 1D version is not able to include iron-oxide compounds for a given elemental depth distribution, which could be a reason for the overestimation of the sputtering yields even in steady state.

The SDTrimSP-2D simulation in addition also includes the initial surface morphology and all dynamically changes during simulated ion irradiation, which leads to an almost perfect agreement with the experimental data. Both the steady state sputtering yield of 1.5 Fe atoms per incident Ar ion as well as the transient effects at very low fluences are very well reproduced.

In Fig. 6 experimental data for the measured and simulated Fe sputtering yields as a function of nominal impact angle are compared for two cases: The green triangles show the situation of the initial target. In addition to the full dynamic SDTrimSP-2D results also data obtained with the 1D version of SDTrimSP are compared, assuming a pure and perfectly flat Fe target, as well as including the elemental depth concentration of the sample. Neither the absolute value nor the qualitative characteristic of the angular dependence can be reproduced correctly with the 1D simulation, while agreement with the 2D version

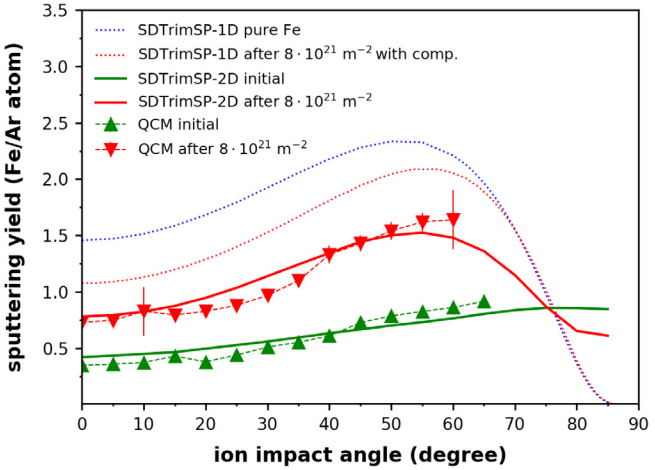

Fig. 6. The green triangles give the measured Fe sputtering yield as a function of nominal impact angle for the initial target surface. A simulation with SDTrimSP-2D (green curve) which includes both the measured surface roughness (from AFM) and elemental composition (from XPS) fits the experimental data better than a static 1D simulation with SDTrimSP assuming a flat surface and a pure Fe target (blue dotted curve). The agreement remains excellent when comparing the experimental data for the Fe film (red inverted triangles) irradiated with a total Ar fluence of 8 × 10^{21} m^{-2} with a fully dynamic SDTrimSP-2D simulation starting from the initial situation given in Fig. 4a. The SDTrimSP-1D simulation, which includes also the elemental depth composition with a flat surface (red dotted line) show a good qualitative agreement, but the absolute values are too high.

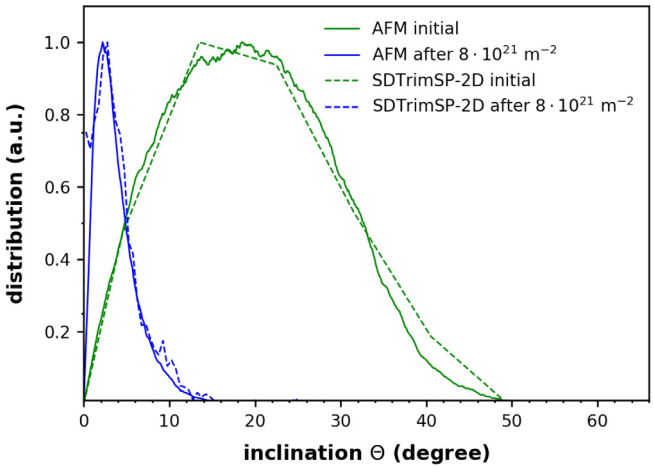

Fig. 7. The distributions of local impact angle θ (i.e. the angles between the direction of the incident projectile and the local surface normal) as derived from the AFM images in Fig. 4, show a shift towards lower angles and a decrease in width after ion-beam irradiation. The dashed lines show the results of numerical simulations with SDTrimSP-2D.

is excellent. It is interesting to see that SDTrimSP-2D predicts even at gracing incidence angles high sputtering yields, but this could not be confirmed due to setup limitations.

After a total Ar fluence of 8 × 10^{21} m^{-2}, applied under an angle of incidence of 60 degrees, the agreement with SDTimSP-2D remains excellent. Here the SDTrimSP-1D simulation, which includes also the elemental depth composition but assumes a flat surface, gives a good qualitative agreement with the measurement, but the absolute values of the sputtering yield are too high. This indicates an ion induced smoothening of the surface, which is confirmed by the AFM measurements (Fig. 3).

The root mean square (RMS) roughness, evaluated from the AFM measurements, shows a decrease from about 5.2 nm (Fig. 3a) to 3.5 nm (Fig. 3b). The RMS roughness value from SDTrimSP-2D gives 3.6 nm (Fig. 4b) and confirms the AFM measurements also very well. This smoothing can much better be quantified by the distribution of the local impact angle θ. This distribution can be evaluated also from the AFM data and a comparison between this distribution of angles before and after irradiation is shown in Fig. 7.

The distribution of the initial rough surface has a peak at around 20 degrees and is very broad, with a full-width-half-maximum (FWHM) of 28 degrees. The distribution after the irradiation has a peak at 2 degrees and a FWHM of 4 degrees. As a perfectly flat surface would be represented by a delta distribution at 0 degrees, the surface can be interpreted as much smoother after the ion irradiation. Fig. 7 also shows the initial local angular distribution of the unirradiated model surface for SDTrimSP-2D (Fig. 4a), which was chosen to match the real surface, evaluated with AFM (Fig. 3a). After a simulated irradiation with Ar by 8 × 10^{21} m^{-2} under 60 degrees, the calculated angular distribution narrows to a FWHM of 4 degrees and has its maximum also at 2 degrees. The smoothing is thus confirmed by SDTrimSP-2D. The remaining small discrepancies between measurement and simulation are probably due to the two dimensional approach. The missing extra dimension reduces possible local impact angles in this dimension, so the local impact angle statistics show also a peak at 0 degrees.

5. Summary and outlook

Sputtering experiments of Fe samples have been performed by using a highly sensitive quartz crystal microbalance technique and compared to BCA simulations with the codes SDTrimSP-1D and SDTrimSP-2D. Monoenergetic Ar ions at 500 eV were used to irradiate the samples under an angle of incidence of 60 degrees.

Sputter XPS measurements of the unirradiated samples showed a clear oxide layer on top and an Fe concentration of only 85% with substantial impurities of O, N and C in the bulk.

AFM measurements before and after irradiation with a total Ar fluence of $8 \times 10^{21}\,m^{-2}$ give information about the change in surface morphology, RMS roughness and local impact angle distribution. A clear decrease of the RMS roughness, as well as the width of the local impact angle distribution could be observed. Additionally nano-scale structures, oriented in the direction of the incident ion beam could be seen.

SDTrimSP-1D simulations assuming a pure elemental target and a perfectly flat surface were not able to reproduce the sputtering behaviour. Including the elemental depth composition into SDTrimSP-1D improved the qualitative agreement at least for the angular dependent sputtering behaviour of the irradiated sample. Only by considering the actual surface structure and elemental composition, including the correct compound information in an SDTrimSP-2D simulation, a close agreement between simulation and experiment could be achieved.

While a two dimensional modelling with SDTrimSP-2D is already quite successful, a full 3D code, called SDTrimSP-3D is under development at IPP and promises even better results [26]. It should include effects like formation of ripple-like structures and will allow investigation of their influence on the sputtering behaviour.

Acknowledgments

The authors are grateful to Michael Schmid (IAP, TU Wien) for his continued support with the QCM electronics. This work has been carried out within the framework of the EUROfusion Consortium and has received funding from the Euratom research and training programme 2014–2018 under Grant agreement No. 633053. The views and opinions expressed herein do not necessarily reflect those of the European Commission. Financial support has also been provided by KKKÖ (commission for the coordination of fusion research in Austria at the Austrian Academy of Sciences – ÖAW).

The computational results presented have been achieved using the Vienna Scientific Cluster (VSC).

References

[1] H. Bolt, V. Barabash, G. Federici, J. Linke, A. Loarte, J. Roth, K. Sato, Plasma facing and high heat flux materials – needs for ITER and beyond, J. Nucl. Mater. 307–311 (Part 1) (2002) 43–52, http://dx.doi.org/10.1016/S0022-3115(02)01175-3.

[2] B. Hapke, Space weathering from Mercury to the asteroid belt, J. Geophys. Res.-Planet. 106 (2001) 10039–10073, http://dx.doi.org/10.1029/2000je001338.

[3] E. Grün, M. Horanyi, Z. Sternovsky, The lunar dust environment, Planet. Space Sci. 59 (2011) 1672–1680, http://dx.doi.org/10.1016/j.pss.2011.04.005.

[4] P. Norajitra, L. Bühler, U. Fischer, S. Gordeev, S. Malang, G. Reimann, Conceptual design of the dual-coolant blanket in the frame of the EU power plant conceptual study, Fusion Eng. Des. 69 (2003) 669–673, http://dx.doi.org/10.1016/S0920-3796(03)00207-2.

[5] K. Sugiyama, J. Roth, V.K. Alimov, K. Schmid, M. Balden, S. Elgeti, F. Koch, T. Hoschen, M.J. Baldwin, R.P. Doerner, H. Maier, W. Jacob, Erosion study of Fe-W binary mixed layer prepared as model system for RAFM steel, J. Nucl. Mater. 463 (2015) 272–275, http://dx.doi.org/10.1016/j.jnucmat.2014.11.044.

[6] B.M. Berger, R. Stadlmayr, D. Blöch, E. Gruber, K. Sugiyama, T. Schwarz-Selinger, F. Aumayr, Erosion of Fe-W model system under normal and oblige D ion irradiation, Nucl. Mater. Energy 12 (2017) 468–471, http://dx.doi.org/10.1016/j.nme.2017.03.030.

[7] P. Sigmund, Theory of Sputtering. I. Sputtering Yield of Amorphous and Polycrystalline Targets, Phys. Rev. 184 (1969) 383–416, http://dx.doi.org/10.1103/PhysRev. 184.383.

[8] A. Mutzke, R. Schneider, W. Eckstein, R. Dohmen, SDTrimSP Version 5.00, IPP-Report 12/8, Max-Planck-Institut für Plasmaphysik, 2011.

[9] R. Behrisch, W. Eckstein, Sputtering by Particle Bombardment, Springer, Berlin Heidelberg, 2007.

[10] M. Küstner, W. Eckstein, V. Dose, J. Roth, The influence of surface roughness on the angular dependence of the sputter yield, Nucl. Instrum. Methods B 145 (1998) 320–331, http://dx.doi.org/10.1016/S0168-583x(98)00399-1.

[11] M. Küstner, W. Eckstein, E. Hechtl, J. Roth, Angular dependence of the sputtering yield of rough beryllium surfaces, J. Nucl. Mater. 265 (1999) 22–27, http://dx.doi.org/10.1016/S0022-3115(98)00648-5.

[12] A. Mutzke, R. Schneider, G. Bandelow, SDTrimSP-2D: Simulation of Particles Bombarding on a Two Dimensional Target-Version 2.0, IPP Report 12/11, Max-Planck-Institut für Plasmaphysik, 2013.

[13] A. Mutzke, I. Bizyukov, R. Schneider, J. Davis, Nano-scale modification of 2D surface structures exposed to 6keV carbon ions: experiment and modeling, Nucl. Instr. Methods Phys. Res. B 269 (2011) 582–589, http://dx.doi.org/10.1016/j.nimb.2011.01.012.

[14] B.M. Berger, R. Stadlmayr, G. Meisl, M. Čekada, C. Eisenmenger-Sittner, T. Schwarz-Selinger, F. Aumayr, Transient effects during erosion of WN by deuterium ions studied with the quartz crystal microbalance technique, Nucl. Instrum. Methods Phys. Res. B 382 (2016) 82–85, http://dx.doi.org/10.1016/j.nimb.2016.04.060.

[15] G. Hayderer, M. Schmid, P. Varga, H.P. Winter, F. Aumayr, A highly sensitive quartz-crystal microbalance for sputtering investigations in slow ion-surface collisions, Rev. Sci. Instrum. 70 (1999) 3696–3700, http://dx.doi.org/10.1063/1.1149979.

[16] K. Dobes, V. Smejkal, T. Schafer, F. Aumayr, Interaction between seeding gas ions and nitrogen saturated tungsten surfaces, Int. J. Mass Spectrom. 365 (2014) 64–67, http://dx.doi.org/10.1016/j.ijms.2013.11.015.

[17] A. Kallenbach, M. Balden, R. Dux, T. Eich, C. Giroud, A. Huber, G.P. Maddison, M. Mayer, K. McCormick, R. Neu, T.W. Petrie, T. Putterich, J. Rapp, M.L. Reinke, K. Schmid, J. Schweinzer, S. Wolfe, A.U. Team, D.-D. Team, A. Team, J.-E. Contributors, Plasma surface interactions in impurity seeded plasmas, J. Nucl. Mater. 415 (2011) S19–S26, http://dx.doi.org/10.1016/j.jnucmat.2010.11.105.

[18] P. Karmakar, D. Ghose, Ion beam sputtering induced ripple formation in thin metal films, Surf Sci. 554 (2004) L101–L106, http://dx.doi.org/10.1016/j.susc.2004.02.020.

[19] W. Eckstein, The Binary Collision Model, in: Computer Simulation of Ion-Solid Interactions, Springer Berlin Heidelberg, Berlin, Heidelberg, 1991 pp. 4–32.

[20] W. Moller, W. Eckstein, Tridyn – a trim simulation code including dynamic composition changes, Nucl. Instrum. Methods B 2 (1984) 814–818, http://dx.doi.org/10.1016/0168-583x(84)90321-5.

[21] W. Moller, W. Eckstein, J.P. Biersack, Tridyn – binary collision simulation of atomic-collisions and dynamic composition changes in solids, Comput. Phys. Commun. 51 (1988) 355–368 10.1016/0010-4655(88)90148-8.

[22] H. Hofsäss, K. Zhang, A. Mutzke, Simulation of ion beam sputtering with SDTrimSP, TRIDYN and SRIM, Appl. Surf. Sci. 310 (2014) 134–141, http://dx.doi.org/10.1016/j.apsusc.2014.03.152.

[23] K. Sugiyama, K. Schmid, W. Jacob, Sputtering of iron, chromium and tungsten by energetic deuterium ion bombardment, Nucl. Mater. Energy 8 (2016) 1–7, http://dx.doi.org/10.1016/j.nme.2016.05.016.

[24] I. Bizyukov, A. Mutzke, R. Schneider, J. Davis, Evolution of the 2D surface structure of a silicon pitch grating under argon ion bombardment: Experiment and modeling, Nucl. Instrum. Methods Phys. Res. B 268 (2010) 2631–2638, http://dx.doi.org/10.1016/j.nimb.2010.06.035.

[25] J. d'Ans, E. Lax, Taschenbuch für Chemiker und Physiker: Band 3: Elemente, anorganische Verbindungen und Materialien, Minerale, Springer-Verlag, 2013.

[26] U.V. Toussaint, A. Mutzke, A. Manhard, Sputtering of rough surfaces: a 3D simulation study, Phys. Scripta 2017 (2017), http://dx.doi.org/10.1088/1402-4896/aa90be 014056.